

WHEEL VIBRATION ANALYSIS FOR INDIRECT TYRE PRESSURE MONITORING SYSTEMS

Péter Gurin 

associate professor, University of Pannonia, Faculty of Engineering, Center for Natural Sciences,
8200 Veszprém, Egyetem u. 10., e-mail: gurin.peter@mk.uni-pannon.hu

Szabolcs Varga 

associate professor, University of Pannonia, Faculty of Engineering, Center for Natural Sciences,
8200 Veszprém, Egyetem u. 10., e-mail: varga.szabolcs@mk.uni-pannon.hu

Abstract

It is evident that tyre pressure has an important impact on driving safety, fuel consumption and driving dynamics. Both direct and indirect tyre pressure monitoring systems have evolved recently, but the direct systems are far more expensive. The most advanced version of the indirect system is based on the eigenfrequency analysis of the angular velocity of the wheels, therefore the understanding of the tyre vibration is an important issue. In this paper we develop a simulation methodology to study the pressure-dependent tyre vibration behaviour. The aim is to better understand the tyre-rim-axle vibration system, with particular emphasis on the torsional vibration modes of the wheel. The focus is on the pressure-dependent correlation between the natural frequency and amplitude of the wheel vibration and the angular velocity and the longitudinal acceleration of the rim. Thus, we describe the oscillatory behaviour relevant for indirect tyre pressure monitoring systems on a theoretical level.

Keywords: *indirect tyre pressure monitoring systems, tyre models, torsional vibrations of the tyre, vehicle dynamics*

1. Introduction

Several previous studies have shown that tyre pressure is a critical factor for vehicle safety, performance and fuel consumption. It has been estimated that compliance with recommended tyre pressures can reduce CO₂ emissions and fuel consumption by an average of about 2.5% (Kubba and Jiang, 2014), and that the introduction of Tyre Pressure Monitoring Systems (TPMS) in the EU Member States alone could reduce CO₂ emissions by 9.6 million tonnes per year. Moreover, maintaining adequate tyre pressure is essential to ensure optimal driving conditions and reduce the risk of accidents (Reiter and Wagner, 2010). Under-inflated tyres can result in reduced grip and handling, increased braking distances and increased tyre wear. Overinflated tyres can lead to harsher driving, reduced traction and increased tyre wear in the centre of the tread. It is therefore essential that drivers regularly check tyre pressures and keep them at the recommended level for their vehicle. Most drivers neglect to check tyre pressure regularly, therefore the TPMS is necessary, which send a warning signal when necessary.

In general, tyre monitoring systems focus on the measurement of the inflation pressure. Tyre inflation pressure can be monitored either conventionally using air pressure sensors, this is the direct TPMS, or by non-traditional methods using other parameters, this is the indirect TPMS, such as individual measurement of tyre angular velocity and comparison them. Direct TPMS can be battery-powered, an

active system, which is typical of the vast majority of TPMS products on the market, or remote-controlled, a passive system, where the system receives the required power wirelessly, for example by means of an electromagnetic field. A wide range of different direct TPMS types is described by Kubba and Jiang (Kubba and Jiang, 2014). In spite of the fact that many technical issues related to direct TPMS have been solved recently (such as the problems of interference and power supply), these systems have a significant installation disadvantage, as they require a complex wiring network for both power supply and readout, therefore these systems are expensive, complex, and require regular maintenance.

Indirect tyre pressure monitoring systems are an alternative to direct TPMS, which measure the tyre pressure indirectly, but at the cost of accuracy and detection time. The accuracy of the indirect TPMS methods are discussed widely in the literature, see e.g. (Adnan, 2019). A compromise solution can be a hybrid TPMS, i.e. a combination of direct and indirect TPMS using fewer tyre pressure sensors. In the latter, only two diagonally spaced tyres are fitted with both direct and indirect TPMS (Formentin et al., 2021). However, the best price solution is a pure indirect TPMS system, because it uses the speed signals from the anti-lock braking system (ABS) for the estimation of the tyre pressure, therefore there is no additional hardware requirements. Furthermore, indirect TPMS is a low-maintenance, and easy-to-implement system that estimates the tyre pressure using various parameters that are related to the tyre pressure.

The two most important phenomena that depend on wheel pressure during pressure loss are the change in rolling radius and the natural frequency of angular velocity vibrations. During pressure loss in the wheel, the rolling radius of a tyre will change along with its pressure, which will further result in changes in the angular velocity of the wheel. Thus, the low tyre pressure can be monitored by measuring and comparing the angular velocity of the wheels. This method works effectively except when all of the tyres of a car are deflated to the same pressure, which means the sizes of tyres are almost equal and the difference between tyre radiuses cannot be observed.

The most easily exploited phenomenon is the shift in the natural frequency of the angular velocity of the wheels. The angular velocity signal provides information about tyre torsional vibration. The vibrations of the tyre are generally excited by road irregularities, brake torque fluctuations, axle height oscillations, and tyre non-uniformities. The natural frequency of tyre torsional vibration depends on tyre pressure. Currently, the most accurate methods use the Fourier transform and the pressure-dependent natural frequency is obtained using the center of gravity or other methods.

These pressure-dependent properties of tyres mentioned above are not only influenced by the tyre pressure. In particular, the natural frequency of tyres can be influenced by the tyre structure, tyre composition, axle elastic kinematics, etc. Recently, in the development of the indirect TPMS, these influencing factors are determined by various tests and therefore vehicle testing plays an important role in the implementation of the indirect TPMS. In order to reduce testing efforts and to predict the performance of the TPMS, different simulation methods can be used to replace vehicle testing and to investigate influencing factors early in the whole vehicle development process. If vehicle testing can be replaced by simulation or rig testing, the costs of developing the indirect TPMS can be significantly reduced. Moreover, simulation and rig testing can be performed at an early stage of the development process when the available prototype vehicles are limited.

For the virtual development of indirect TPMS, before running virtual tests, it is necessary to clarify which tyre model is suitable for virtual tests and what factors influence the vibration behaviour of the tyre. All the model used can be categorized in three main types.

1. The first category consists of models that describe the behavior of a tyre without a physical basis. Examples include all versions of Magic Formula, TMeasy, TameTyre, MF-Swift, etc. (Hirschberg

et al., 2007; Durand-Gasselín et al., 2010; Pacejka, 2012). These models provide an empirical or mathematical description of the observed properties of tyres, some of which may contain physical relationships to certain properties, for instance, their dependence on temperature. (The TameTyre model lies between category 1 and 2 as it presents a significant amount of physical modeling in the low frequency range.)

2. The next category comprises models that model the tyre based on physical relationships, although these models commonly contain many simplifying assumptions. Examples include first of all the rigid ring tyre model (Zegelaar, 1998; Sivaramakrishnan et al., 2015), then Ftyre (Gipser, 2016; Pacejka, 2012), various versions of CDTyre (Gallrein et al., 2013), and various versions of RMOD-K (Oertel and Wei, 2012). These models use simplification, idealization and discretization, but are still physically consistent models based on the mechanical, thermodynamic and tribological properties of a real tyre.
3. Finally, there is the class of nonlinear finite element models of elasticity. These models are similar to those in the previous category, but are distinguished by four critical features: a lower level of simplification and idealisation of the mechanical structure, longer computation times, the use of multi-purpose FE software, and parameterisation based on initial design and material data rather than tyre tests.

When using simplified models, the small number of parameters in the equations of motion is an obvious advantage over other complex models. This can improve the understanding of tyre vibration behaviour and the investigation of how vibration behaviour is related to certain tyre design parameters. However, a complex model, such as a multi-body model, obviously cannot be fully substituted by a simplified model. A complex model can better describe certain dynamic properties, such as dynamic stiffness and nonlinearity of the elastic elements. Parameterization and validation are two important and non-trivial parts of a reliable model. For this reason, simulation results must be compared with data from the test rig and vehicle tests.

Virtual development is usually divided into three levels: component level, subsystem level and full vehicle level. In this paper we neglect the third one, and focus on the first two level. We will refer to them as the “component” model and the “subsystem” model. In this frame, a simulation methodology is developed here to simulate the pressure-dependent tyre vibration behaviour. The aim is to better understand the wheel-tyre-axle vibration system, with a focus on the longitudinal torsional vibration modes of the wheel. Emphasis will be placed on the pressure-dependent relationship between the longitudinal force on the tyre and the angular velocity of the wheel, and on the interaction between the elastokinematics of the tyre and the elastokinematics of the wheel suspension. Thus the behaviour of vibrations relevant for indirect tyre pressure control systems is described at a theoretical level. Based on the findings in the literature from the test rig measurements and road tests, the first part of the paper (Section 2) deals with the modelling of the tyre as a component, and the modelling of the interaction of the tyre component with the elastokinematics of the wheel suspension. In the second part of the paper (Section 3), the parameterization of the models are presented. The third part presents or results related to the models. Firstly (Section 3) the characteristics of the models are discussed based on the magnitude and phase of their eigenvectors, respectively. In addition, the natural frequencies of the models are analysed as a function of tyre pressure. Then (Section 4) we present the calculation results of the wheel angular velocity as well as the longitudinal acceleration of the rim under a single obstacle excitation. Finally, the results are summarised, in line with the objective of defining a tyre evaluation methodology for the indirect tyre pressure monitoring systems.

2. Tyre models

A component level model of the longitudinal torsional oscillations of the tyre must include the longitudinal forces in addition to the rim rotation. Despite the fact that the tyre is a flexible body, it has been shown in the literature (Zegelaar, 1998; Sivaramakrishnan et al., 2015) that the appropriate behaviour can be realised with a model in which the tyre belt is represented as a rigid ring. This is the so-called rigid ring tyre model, which was proposed firstly in the late 1990s (Zegelaar, 1998) Despite the fact that it is a relatively old publication, it is still considered as a landmark work in the field, it is also the starting point for our work. The rigid ring tyre model is a simplified mathematical representation of the tyre which assumes that the tyre moves as a rigid body relative to the rim. In other words, the model includes only those modes of vibration in which the tyre itself remains rigid and circular. According to the literature, this approximation is suitable to describe vibration modes below 100 Hz (Zegelaar, 1998), which is the most important range for indirect TPMS systems. The tyre belt is connected to the rim by springs and dampers in radial and torsional directions. This is the simplest model that fall into category 2 mentioned in the Introduction. In this work, we use a similar approach to develop the “component” model, whose structure is shown in Figure 1.

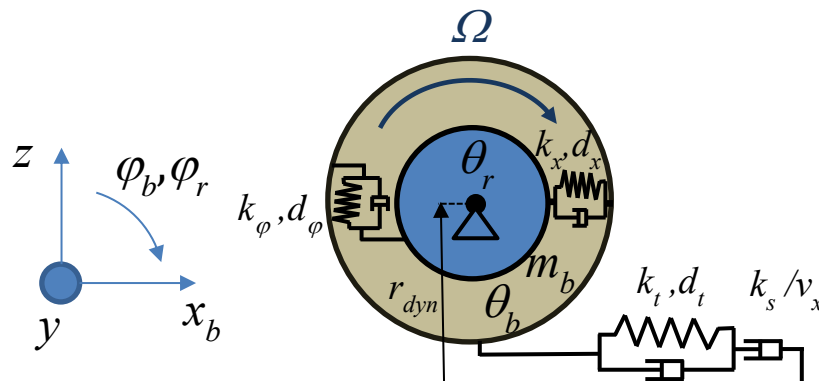


Figure 1. The „component” model

The rim has only one rotational degree of freedom, φ_r , with an associated moment of inertia Θ_r . Thus, the „component” model corresponds to the situation on the tyre test rig with the wheel kinematically fixed in the vertical direction. The tyre belt is modelled as a rigid ring and has a translational degree of freedom x_b as well as a rotational degree of freedom φ_b . Accordingly, the belt as a rigid ring has a mass m_b and a moment of inertia Θ_b . In the longitudinal direction, the ring is coupled to the rim via a stiffness k_x and a damping d_x , which symbolize the sidewall stiffness as well as the damping characteristics of the tyre in the longitudinal direction. Furthermore, the coupling to the rim in circumferential direction is done via a rotational stiffness k_φ and a damping d_φ , which represent the torsional characteristic of the tyre sidewall. An advantage of the rigid ring model is that the sidewall flexibility is directly represented by the degrees of freedom of the tyre belt, x_b and φ_b . With the model approach of a rigid ring, in principle only those tyre modes can be simulated, which can be approximately considered as rigid-body modes, i.e. without deformation of the ring itself. The simulation of higher-frequency tyre modes, in which the tyre belt itself deforms, is not possible with this model approach, since the belt must then be modelled as a flexible element.

As we discuss in detail in the next paragraph, the dynamic transmission behaviour between the tyre and the contact surface under transient slip and wheel load changes can be described by a longitudinal force $F_s = k_s s_x$, where the coupling constant k_s is the slip stiffness, and s_x is the slip, which is a degree of freedom to describe all kinematic information about the relative position of the tyre and the contact surface. Thus, the degrees of freedom of our partial model (that we call “component” model) consists of the rotation of the rim φ_r , the translation x_b and the rotation φ_b of the belt, and finally the slip s_x according to the contact model mentioned above. According to the Newton’s law for rigid bodies, the equations of free motion of the rim and the belt in the absence of external excitations can be written as follows,

$$\begin{aligned}\Theta_r \ddot{\varphi}_r &= -k_\varphi (\varphi_r - \varphi_b) - d_\varphi (\dot{\varphi}_r - \dot{\varphi}_b) \\ \Theta_b \ddot{\varphi}_b &= -k_\varphi (\varphi_b - \varphi_r) - d_\varphi (\dot{\varphi}_b - \dot{\varphi}_r) - k_s s_x r_{dyn} \\ m_b \ddot{x}_b &= -k_x x_b - d_x \dot{x}_b + k_s s_x.\end{aligned}\quad (1)$$

According to Zegelaar (Zegelaar, 1998), who is the founding father of the rigid ring tyre model, the dynamic behaviour of the tyre-surface interaction can be described by a contact model which is represented by a first-order linear system. The time constant of the first order system corresponds to the ratio of relaxation length and translational velocity, σ / v_x , and the amplification factor corresponds to the ratio of slip stiffness and translational velocity, k_s / v_x . Here the relaxation length σ is the distance travelled after a sudden change in the input variable until 63% of the steady-state final value is reached. The translational velocity, or rolling speed, v_x , is related to the angular velocity of the wheel, Ω ,

$$v_x = r_{dyn} \Omega, \quad (2)$$

where r_{dyn} is the dynamic rolling radius which is a constant. The slip velocity, v_s , is given by the difference between the translational velocity of the ring and its circumferential velocity according to the following equation,

$$v_s = \dot{x}_b - r_{dyn} (\dot{\varphi}_b - \Omega). \quad (3)$$

Actually, v_s is the velocity of the tyre in the contact zone, and it is the system input of the contact model. By definition, the slip velocity is positive and the slip is negative if the translational velocity of the ring is greater than its circumferential velocity. The other variables in the contact model definition are the tread stiffness k_t and the tread damping d_t (for variables see Fig. 1). Using these variables the dynamic equation for describing the slip according to the above described contact model is given by the following equation,

$$\left(\sigma + \frac{d_t}{k_t} |v_x| \right) \dot{s}_x + |v_x| s_x = -v_s - \frac{d_t}{k_t} \dot{v}_s. \quad (4)$$

An advantage of the formulation of the contact model according to equation (4) is that the slip definition is not directly included. Zegelaar has also shown that the first-order system for longitudinal slip s_x according to equation (4), taking into account the flexibility of the wall, is best suited for implementation in the tyre model (in terms of slip and wheel load variation and numerical stability).

Thus finally, the equations of motion describing the free oscillations of the model, taking into account also the contact model, are given by equations (1) and (4). To study the natural frequencies and the

corresponding oscillation modes of the system it is convenient to write these equations of motion as a system of first order linear differential equations as follows,

$$\dot{\xi}_c = A_c \xi_c + B_c. \quad (5)$$

Here, ξ_c denotes the state vector containing the state variables of the “component” model,

$$\xi_c = (\varphi_r, \varphi_b, x_b, s_x, \dot{\varphi}_r, \dot{\varphi}_b, \dot{x}_b)^\top, \quad (6)$$

and the definitions of the A_c and B_c matrices are obvious based on the equations of motion (1) and (4), furthermore substituting the definition of v_s from equation (3) into equation (4):

$$A_c = \begin{pmatrix} 0 & 0 & 0 & 0 & 1 & 0 & 0 \\ 0 & 0 & 0 & 0 & 0 & 1 & 0 \\ 0 & 0 & 0 & 0 & 0 & 0 & 1 \\ -\frac{k_\varphi r_{dyn}}{\Theta_b a} & \frac{k_\varphi r_{dyn}}{\Theta_b a} & \frac{k_x}{m_b a} & \frac{k_s}{a} \left(\frac{r_{dyn}^2}{\Theta_b} - \frac{1}{m_b} \right) - \frac{k_t |v_x|}{d_t a} & -\frac{d_\varphi r_{dyn}}{\Theta_b a} & \frac{d_\varphi r_{dyn}}{\Theta_b a} + \frac{k_t r_{dyn}}{d_t a} & \frac{d_x}{m_b a} - \frac{k_t}{d_t a} \\ -\frac{k_\varphi}{\Theta_r} & \frac{k_\varphi}{\Theta_r} & 0 & 0 & -\frac{d_\varphi}{\Theta_r} & \frac{d_\varphi}{\Theta_r} & 0 \\ \frac{k_\varphi}{\Theta_b} & -\frac{k_\varphi}{\Theta_b} & 0 & -\frac{k_s r_{dyn}}{\Theta_b} & \frac{d_\varphi}{\Theta_b} & -\frac{d_\varphi}{\Theta_b} & 0 \\ 0 & 0 & -\frac{k_x}{m_b} & \frac{k_s}{m_b} & 0 & 0 & -\frac{d_x}{m_b} \end{pmatrix} \quad (7)$$

and

$$B_c = \begin{pmatrix} 0 & 0 & 0 & -\frac{k_t |v_x|}{d_t a} & 0 & 0 & 0 \end{pmatrix}^\top \quad (8)$$

where

$$a = \left(\frac{k_t}{d_t} \sigma + |v_x| \right). \quad (9)$$

Furthermore, for performing time step simulations with arbitrary excitation characteristics an extra term must be added to the right hand side of equation (5), η_c , which describe the excitation. The definition of the excitation in the simulation of a vehicle rolling over a single cleat is discussed in more detail in the Subsection 5.1.

As mentioned above, the second partial model, that we call “subsystem” model, is developed to analyse the interaction between the tyre as a component and the elastokinematics of the wheel suspension on a general, fundamental level. Fig. 2 shows the structure of the “subsystem” model. It can be seen that the basic model structure is identical to the “component” model. In the “subsystem” model, the ring (belt) also has a translational degree of freedom x_b (in the longitudinal direction) and a rotational degree of freedom φ_b , and it is coupled to the rim and to the ground.

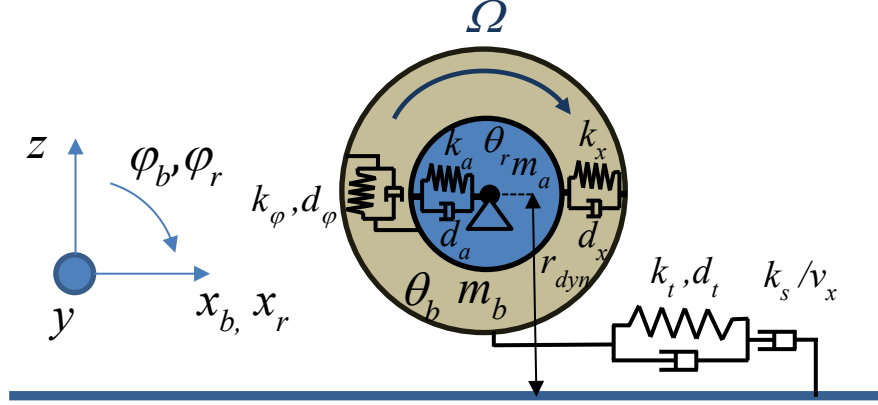


Figure 2. The “subsystem” model

The contact model is also the same as in the case of the “component” model. The difference lies in an additional degree of freedom x_r of the rim in longitudinal direction, which is coupled to the fixed environment described by a stiffness k_a and the damping d_a . This additional degree of freedom symbolizes the generalized translational longitudinal elasticity of the front axle suspension. Consequently, a mass m_a is also defined, which represents the oscillatory mass of the wheel suspension. The model structure corresponds (neglecting the vertical direction) in the broadest sense to the situation on the wheel-axle test rig and, neglecting the vehicle body mass, to the situation in the road test. In the case of the rear axle, the elastically mounted subframe must be taken into account. The neglecting of the vehicle body mass is permissible because the vehicle body mass is significantly higher than the oscillating masses considered here.

Thus, the degrees of freedom of the “subsystem” model consists of the translation x_r and the rotation φ_r of the rim, the translation x_b and the rotation φ_b of the belt as well as the slip s_x according to the contact model. The linear equations of motion of the model which describe the free oscillations are given by equations (4) and (10):

$$\begin{aligned} \Theta_r \ddot{\varphi}_r &= -k_\varphi (\varphi_r - \varphi_b) - d_\varphi (\dot{\varphi}_r - \dot{\varphi}_b) \\ m_a \ddot{x}_r &= -k_x (x_r - x_b) - k_a x_r - d_x (\dot{x}_r - \dot{x}_b) - d_a \dot{x}_r \\ \Theta_b \ddot{\varphi}_b &= -k_\varphi (\varphi_b - \varphi_r) - d_\varphi (\dot{\varphi}_b - \dot{\varphi}_r) - k_s s_x r_{dyn} \\ m_b \ddot{x}_b &= -k_x (x_b - x_r) - d_x (\dot{x}_b - \dot{x}_r) + k_s s_x. \end{aligned} \quad (10)$$

Analogous to the „component” model, the equations of motion of the „subsystem” model can be written as a system of first order linear differential equations,

$$\dot{\xi}_s = A_s \xi_s + B_s. \quad (11)$$

Certainly, due to axle elasticity the state vector ξ_s is extended by the additional state variables, the translational position of the rim, x_r , and translational velocity of the rim, \dot{x}_r ,

$$\xi_s = (\varphi_r, \varphi_b, x_r, x_b, s_x, \dot{\varphi}_r, \dot{\varphi}_b, \dot{x}_r, \dot{x}_b)^\top. \quad (12)$$

This also changes the definition of the matrices A_s and B_s in a straightforward way since the derivation of these matrices is based on the equations of motion.

3. Parameterization of the models

Both simulation models are designed as linear models. However, this does not agree with the real physical system, since in principle all parameters occur nonlinearly. As an example, the generalized axle stiffness and axle damping of the front axle shall be given. It is significantly influenced by the characteristics of the bearings, whose stiffness and damping are frequency-dependent and therefore represent nonlinear force elements. Based on measurements published in the literature (see e.g. Pfeffer and Hofer, 2002), Figure 3 shows the typical behaviour of the normalized dynamic stiffness and the normalized damping angle (sometimes called loss angle) of the bearing as a function of frequency. It can be seen that the damping maximum of the bearing is designed for the range of the axis longitudinal natural frequency at about 13-15 Hz in order to damp this natural vibration for comfort reasons. In the range of the torsional longitudinal tyre vibration (30-40 Hz) the damping angle is approx. 50% lower. Due to their design, the dynamic stiffness increases sharply in the region of the damping maximum. This means that the dynamic stiffness in the area of the axis natural frequency is only around one third of the stiffness in the area of the torsional longitudinal tyre vibration.

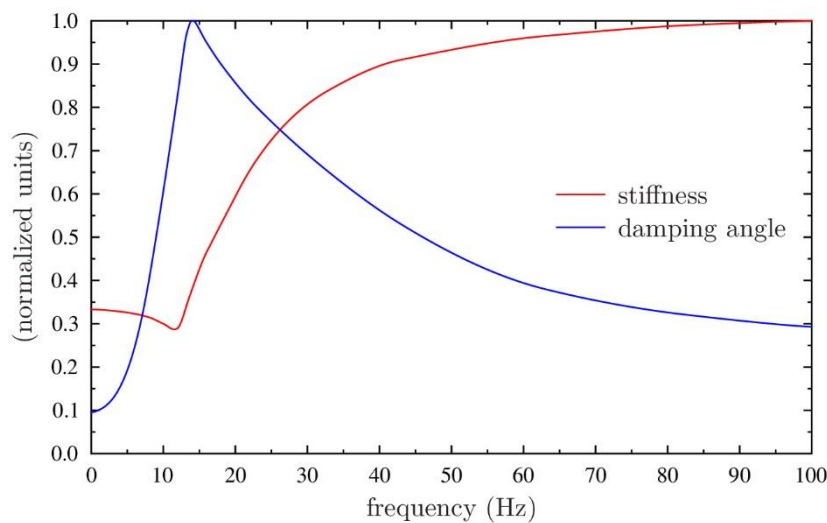


Figure 3. Typical behaviour of the normalized dynamic stiffness (red line) and the normalized damping angle (blue line) of the bearing as a function of frequency

For the parameterization of the linear models, this results in the fact that the representation of the generalized longitudinal stiffness of the axle with a linear stiffness and a linear damper is actually not possible. One possible solution to this problem is to represent the frequency-dependent stiffness and damping of elastomeric or hydromounts with suitable mechanical substitute models. Approaches for the representation of conventional elastomeric bearings as well as of hydromounts are presented by Pfeffer and Hofer (Pfeffer and Hofer, 2002), among others. For the derivation of principle statements

concerning the interaction between the tyre and the chassis elasticity, the consideration of a constant stiffness or a constant damping is sufficient in this work. Using the above example of longitudinal axle elasticity, it becomes clear that the real parameters of the simulation models are partly subject to strong nonlinearities, which leads to simulation results that are not valid for the whole working range of the tyre, but only in the vicinity of a certain working point. However, in Subsection 5.2 we examine the effect of axle elasticity on our results, and we find that the results are robust against the changing of this parameter.

Table 1 contains the complete set of parameters of both models with symbol and unit for three different tyre pressures “Pressure 1”, “Pressure 2” and “Pressure 3”, where the first one represents the highest and the last the lowest tyre pressure.

Table 1. Parameter set of the models for the simulations

symbol	parameter (unit)	Pressure 1	Pressure 2	Pressure 3
m_b	mass of the vibrating tyre belt (kg)	7.1	6.9	6.7
Θ_b	moment of inertia of the vib. tyre belt (kg/m ²)	0.69	0.67	0.65
m_a	mass of the oscillating axle (kg)	35	35	35
Θ_r	moment of inertia of the rim (kg/m ²)	0.68	0.68	0.68
k_x	longitudinal tyre stiffness (N/m)	$1.5 \cdot 10^6$	$1.4 \cdot 10^6$	$1.3 \cdot 10^6$
k_φ	tyre torsional stiffness (Nm/rad)	$78 \cdot 10^3$	$74 \cdot 10^3$	$70 \cdot 10^3$
k_t	tread stiffness (N/m)	$1.55 \cdot 10^6$	$1.6 \cdot 10^6$	$1.65 \cdot 10^6$
k_s	slip stiffness (N)	$185 \cdot 10^3$	$190 \cdot 10^3$	$195 \cdot 10^3$
k_a	axle longitudinal stiffness (N/m)	$350 \cdot 10^3$	$350 \cdot 10^3$	$350 \cdot 10^3$
d_x	longitudinal tyre damping (Ns/m)	290	260	230
d_φ	torsional tyre damping (Nm s/rad)	13	12	11
d_t	tread damping (Ns/m)	180	220	260
d_a	axle longitudinal damping (Ns/m)	3500	3500	3500
r_{dyn}	dynamic rolling radius (m)	0.35	0.345	0.34
σ	relaxation length (m)	0.09	0.95	0.1
v_x	rolling speed (m/s)	10	10	10

Only qualitative information is introduced for the tyre pressures, since the parameterization is not based on the behavior of a specific tyre at well-defined tyre pressures. The concrete parameter values are partly based on measurements (such as weight, mass inertias and cleat test measurements) and partly represent assumptions. The choice of parameter values was based mainly on the works of Schmeitz (Schmeitz, 2004; Schmeitz et al., 2005).

The mass parameters m_b and Θ_b of the tyre belt are defined with decreasing values as the tyre pressure decreases, because the reduced vertical stiffness increases the fixation of the tyre to the ground. This means that more of the tyre is bound to the contact patch and the vibrating part of the belt is reduced. In contrast, the mass parameters of the axle or rim m_a and Θ_r are not affected by the tyre pressure. The same moment of inertia is defined for the rim in both models.

The longitudinal tyre stiffness k_x as well as the longitudinal tyre damping d_x are defined as decreasing with decreasing tyre pressure due to the decreasing tension of the tyre as a result of the lower compressed air content in the tyre. The same applies (in an identical manner) to the torsional tyre elasticity consisting of the stiffness k_φ and the damping d_φ . The effective tread stiffness k_t and the tread damping d_t depend significantly on the size of the contact patch, which increases with decreasing tyre pressure due to decreasing vertical stiffness (Doria and Taraborrelli, 2016). It follows that the effective tread stiffness and the corresponding damping increase with decreasing tyre pressure.

Based on the results of Schmeitz et al. (Schmeitz et al., 2005), the longitudinal slip stiffness increases with decreasing tyre pressure and with increasing wheel load for a tested tyre in the dimension 225/55 R16. The main reason for this is the extended contact patch. Therefore the slip stiffness k_s is defined in this work as increasing with decreasing tyre pressure. In correlation with the measurement results of the transverse dynamic relaxation length as a function of tyre pressure (Doria and Taraborrelli, 2016), the longitudinal relaxation length σ increases with decreasing tyre pressure. In contrast, the generalized axial elasticity with stiffness k_a and damping d_a is constant over the tyre pressure.

4. Free response characteristics of the models

In this Section the description and discussion of the model characteristics of both models are given. The imaginary part of the eigenvalues of the matrices A_c and A_s gives the natural frequencies of the corresponding models. Table 2 shows the free response model characteristics of the “component” model on the basis of amplitude (absolute value) and phase of the complex eigenvectors in the parameterization for “Pressure 1”. In addition, the corresponding natural frequencies are also contained.

For the “component” model, three eigenvalues result from the three mass parameters. The first eigenmode corresponds to the torsional longitudinal tyre mode and has an associated natural frequency of 34.93 Hz. From the phase information it can be seen that for this mode of vibration the degrees of freedom φ_r , x_b and φ_b are approximately in phase. The characteristics of this oscillation mode correlate with the results of Zegelaar (Zegelaar, 1998), who, among others, calls this oscillation mode “in-phase rotational mode”, in which tyre and rim oscillate in the same phase. From the magnitudes of the eigenvector components it can be seen that the rotational vibration amplitudes of the tyre belt are lower compared to that of rim.

In contrast to the first eigenmode, the second eigenmode at 74.82 Hz is characterized by the antiphase of rim rotation and belt motion. A corresponding behaviour is also found in the literature (see e.g. Zegelaar, 1998). It is called “anti-phase rotational mode”, and identified as the second mode of vibration,

in which the vibrations of rim and belt oscillate in antiphase. The magnitude information of the eigenvector components show that in this mode the amplitudes of the rim rotation are comparable to those of the belt rotation.

Table 2. Relevant components of the eigenvectors and corresponding natural frequencies of the “component” model at “Pressure 1”. The eigenvectors are normalized in such a way that the largest component is 1

natural frequency (Hz)	φ_r		φ_b		x_b	
	Amplitude	Phase	Amplitude	Phase	Amplitude	Phase
$f_1 = 34.93$	1	-93.32°	0.58	-96.63°	0.13	-89.09°
$f_2 = 74.82$	1	-92.44°	0.93	88.35°	0.34	81.42°
$f_3 = 143.46$	0.16	-92.04°	1	86.37°	0.31	-92.97°

The third eigenmode of the “component” model has a natural frequency of 143.46 Hz. From the phase information of the associated eigenvector it can be seen that this oscillatory mode is characterized by the opposite phase of translation and rotation of the belt. As in the second eigenmode, the rotation of the rim is in opposite phase compared to that of belt rotation. However, in contrast to the second oscillatory mode, the belt rotation occurs with higher amplitudes than the rim rotation.

Based on the experimental results from the literature which are related to the situation on the tyre test rig with the wheel kinematically fixed in the vertical direction (see e.g. Zegelaar, 1998; Schmeitz, 2004; Pacejka, 2012) we can say that the typical amplitude spectra of the wheel angular velocity (in the case of a single cleat excitation) has two eigenfrequencies in the frequency range up to 120 Hz. The first resonance point is the torsional longitudinal tyre mode with the already known pressure-dependent behaviour, typically in the range of 30-40 Hz. The second resonance frequency is in the range of 70-80 Hz with identical pressure-dependent characteristics. These are good agreement with our results. However, in the literature, besides the data for the angular velocity spectrum, there are data for the amplitude spectra of the longitudinal tyre force, in which a third resonant frequency in the range of approx. 100 Hz can also be detected. A natural question arises about the origin of this belt vibration. The comparison with our results (see Table 2) shows no corresponding natural frequency. According to the selected model approach, however, rotational vibrations of the rim and vibrations of the belt always occur together with a defined coupling. Based on this, it can be concluded that the vibration mode in the range of 100 Hz represents a flexible belt mode, which cannot be represented by the model approach chosen here. Also Schmeitz determines a third peak at approx. 110 Hz (Schmeitz, 2004) beside the “in-phase” mode at 35 Hz and the “anti-phase” mode at 80 Hz, which are both visible in the tyre longitudinal force and the wheel angular velocity. However, in his opinion, this frequency is attributed to the structural dynamics of the test rig. Zegelaar (Zegelaar, 1998) also determines, in addition to the “in-phase” and the “anti-phase” mode, which are both visible in the tyre longitudinal force and the wheel angular velocity, a third oscillation which only occurs in the tyre longitudinal force. According to Zegelaar, this represents the first flexible belt mode, which has a higher natural oscillation frequency of 90 Hz compared to the “anti-phase” mode. We agree with this opinion.

In analogy to the “component” model, the model characteristic of the “subsystem” model is also analysed. Table 3 shows absolute value and phase of the complex eigenvectors and the corresponding four natural frequencies at the highest tyre pressure (“Pressure 1”).

Table 3. Relevant components of the eigenvectors and corresponding natural frequencies of the “subsystem” model at “Pressure 1”. The eigenvectors are normalized in such a way that the largest component is 1

natural frequency (Hz)	φ_r		x_r		φ_b		x_b	
	Amp.	Phase	Amp.	Phase	Amp.	Phase	Amp.	Phase
$f_1 = 11.77$	1	-112.73°	0.31	-118.5°	0.96	-115.1°	0.32	-114.97°
$f_2 = 41.54$	1	-96.51°	0.1	99.87°	0.42	-111.72°	0.05	-118.83°
$f_3 = 77.76$	0.91	-95.16°	0.074	-86.56°	1	87.08°	0.33	79.38°
$f_4 = 143.96$	0.16	-92.21°	0.018	96.67°	1	86.31°	0.32	-92.79°

The first calculated natural mode at 11.77 Hz represents an in-phase oscillation of all four degrees of freedom. This means that the wheel angular velocity oscillate in phase with the translational motion of the masses coupled to the rim. This represents a very good correlation to the measurement results on the wheel-axle test rig, since the axle natural oscillation as the first identified oscillation also represents an in-phase oscillation of axle longitudinal motion and tyre longitudinal force (Zegelaar, 1998; Schmeitz, 2004). From the magnitude it can be seen that both rotational degrees of freedoms as well as both translational degrees of freedoms occur with comparable amplitudes.

In correlation to the measurement results on the wheel-axle test rig (Zegelaar, 1998; Schmeitz, 2004; Pacejka, 2012), the second natural oscillation corresponds to the torsional longitudinal tyre mode, which results at a frequency of 41.54 Hz. From the phase information it is clear that the interaction with the axle elasticity does not really affect the characteristics of the tyre vibration and that all three degrees of freedom of the tyre still oscillate almost in phase. It follows that there is a strong coupling between the longitudinal acceleration of the rim and the wheel angular velocity, which correlates with the measurement results. Changes in the conditions due to the loss of the pressure in the tyre, are therefore just as observable in the longitudinal acceleration of the rim as in the wheel angular velocity. The counter-phase of the translational motion of the rim in the torsional longitudinal vibration mode of the tyre is also consistent with the measurement results. On the other hand, the additional axle elasticity also results in a shift of the natural frequency of the torsional longitudinal tyre mode to higher frequencies in the model. From the absolute values of the eigenvector components it can be seen that the amplitudes of the translational motions are small and similar, but the amplitude of the rim rotation is higher compared to the tyre belt. The determined model characteristics, especially with respect to the phase relationship between tyre vibration and axle vibration, correlate with the results of Schmeitz (Schmeitz, 2004).

The analysis of the third and fourth natural vibration shows a very high correlation to the second and third natural vibration of the “component” model with respect to the natural frequency and the amplitude

and phase of the degrees of freedom φ_r , x_b and φ_b . The main difference lies in the additional degree of freedom, x_r , which occurs in both eigenmodes in antiphase to the translational belt motion, but has significantly lower amplitudes. It follows that the characteristics of the eigenmodes at the component level are not significantly affected by the interaction with the axial elasticity. Only the natural frequency of the torsional longitudinal tyre mode shifts slightly to higher frequencies, which, according to the literature, can also be observed in an identical way in the measurement data.

5. Simulation of a single cleat crossing

For the simulation of a single cleat crossing, time step simulations was performed with both models. In the following, the external excitation of the state space models for these simulation is discussed. Then the resulting amplitude spectra of the wheel angular velocity and the longitudinal acceleration of the rim are considered at the three different tyre pressures. Direct comparison is always made with the results of the measurements known from the literature. Subsequently, the variation of the axle elasticity is performed in order to determine the influence of the wheel suspension on the sensitivity of the tyre vibrations with respect to the pressure loss.

5.1. Definition of the excitation

As mentioned at the beginning, both models are simulated with an impact excitation by a single cleat. In principle, it is also possible to simulate a stochastic road excitation in addition to the deterministic excitation (Schmeitz, 2004). However, due to the linearity of the two models, in this work the analysis of the simulation results is limited to the deterministic excitation by a single cleat. In the studied case the velocity is $v_x = 36$ km/h (i.e. $v_x = 10$ m/s).

Keeping the model conception of a rigid ring rolling over a single obstacle (cleat), two different torques as well as two forces can generally be identified during the obstacle crossing which realize the vibration excitation. **Hiba! A hivatkozási forrás nem található.** illustrates these forces and torques. When the ring hits the cleat, a vertical force F_z and a longitudinal force F_x occur simultaneously against the direction of motion. In addition, due to the effective lever arms l_x and l_z , two torques about the y-axis $M_y^{(F_x)}$ as well as $M_y^{(F_z)}$ occur according to equation (13) and equation (14).

$$M_y^{(F_x)} = F_x^{cleat} l_z \quad (13)$$

$$M_y^{(F_z)} = F_z^{cleat} l_x \quad (14)$$

It becomes clear that, except for the vertical force F_z , all three excitation variables change sign during the rolling over the cleat when the cleat passes through the tyre center plane.

As we have mentioned, when simulating a single cleat crossing an extra term must be added to the right hand side of equation (5) and (11), η_c , which describe the excitation. From **Hiba! A hivatkozási forrás nem található.** it is clear that in the case of the „component” model,

$$\eta_c = \left(0 \quad 0 \quad 0 \quad 0 \quad 0 \quad M_y^{(F_z)}(t) - M_y^{(F_x)}(t) \quad -F_x^{cleat}(t) \right)^T. \quad (15)$$

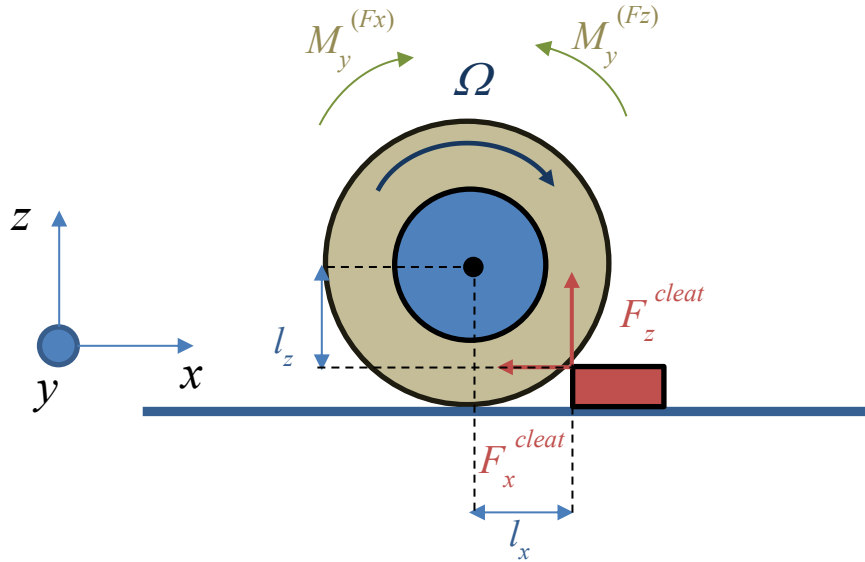


Figure 4. Excitation variables during a single cleat crossing

The case of the “subsystem” model is straightforward.

Since the tyre belt undergoes elastic deformation as it passes through the cleat, the rigid ring model approach is inherently limited in its ability to describe the excitation. Model-based approaches to describe the excitation by a single cleat in a rigid ring model approach are given by Zegelaar (Zegelaar, 1998). Zegelaar presents that the time histories of the tyre forces can be well represented even during the excitation phase. However, the excitation stage is less relevant in the context of this work than the free oscillations after the excitation, therefore a detailed description of the excitation process is omitted, and in our work, for the time evolution of the longitudinal and vertical excitation forces we use the results of Schmeitz et al. (Schmeitz et al., 2005).

Furthermore, the simplifying assumption is made that the excitation characteristic changes only as a function of speed, but are the same for all tyre pressures. However, from the excitation analysis according to the literature (Oertel and Wei, 2012), it follows that the excitation itself is also pressure-dependent, since the effective length of the lever arm changes with the pressure. Thus, the pressure dependence of both models results exclusively from the pressure-dependent tyre characteristic itself.

In the case of the “subsystem” model, besides the angular velocity, we calculate the longitudinal acceleration of the rim, which is also a measurable quantity. It is easy to compute it as the second to last (8th) component of the vector $\dot{\xi}_s$, see equation (12), that is known from equation (11).

5.2. Simulation results

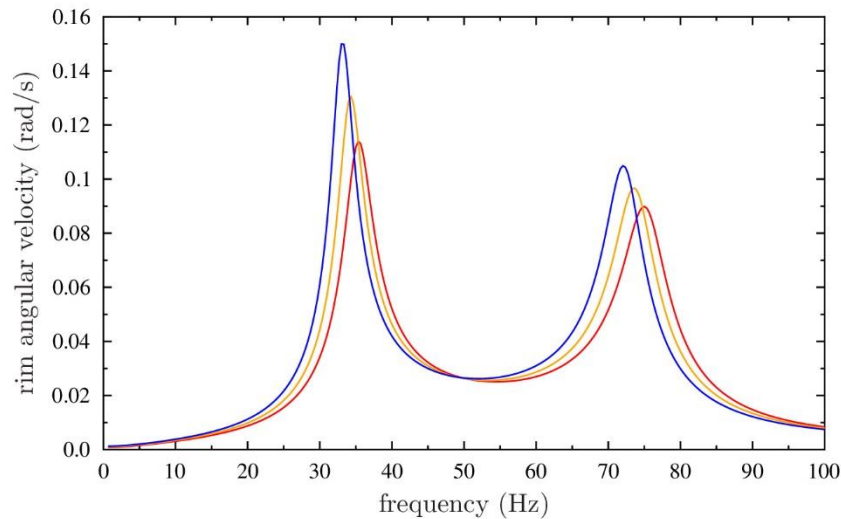


Figure 5. Amplitude spectrum of the wheel angular velocity of the “component” model for a single cleat excitation at 36 km/h

Hiba! A hivatkozási forrás nem található. shows the amplitude spectra of the wheel angular velocity, which are obtained with a single cleat excitation at a speed of 36 km/h for the “component” model. As a result of the specific characteristics of the torsional longitudinal oscillation mode and the corresponding pressure-dependent parameterization, a reduction in the oscillation frequency and an increase in the oscillation amplitude are obtained with decreasing tyre pressure. It is in a complete correlation to the measurement results (Schmeitz, 2004; Pacejka, 2012), thus the behaviour observed in the measurement can be reproduced and understood within the framework of the simple theory to which our calculations refer. However, we should mention that compared to the measured data, the amplitudes are lower, which is partly due to the fact that the parameterization of the model is not optimized for the tyre used in the measurement. On the other hand, it must be taken into account that the amplitudes also deviate from the measured data as a result of the highly simplified excitation definition.

Analogous to the „component” model, the simulation result of the “subsystem” model with a single cleat excitation at a speed of 36 km/h is shown in Figure 6. Based on the amplitude spectra of the wheel angular velocity and the longitudinal acceleration of the rim, it can be seen that the low-frequency vibration is hardly dependent on the tyre pressure as a result of axle elasticity. Only the vibration amplitudes show a very slight change with variation of the tyre pressure.

In contrast, the torsional longitudinal tyre mode shows the familiar and, compared to the wheel-axle test rig, identical pressure-dependent behaviour. With decreasing tyre pressure, the vibration frequencies decrease in both wheel angular velocity and rim acceleration, while the vibration amplitudes increase.

In a similar way like the simulation result of the “component” model, the “subsystem” model shows lower amplitudes compared with the measurement (on the wheel-axle test rig). For this the reasons are also similar: the parameterization, which is not optimized for the tyre used in the measurement, and the

greatly simplified definition of the excitation. Overall, the “subsystem” model also shows a very good correlation with the measured data.

It is important to note that our simulation results show that the anti-phase torsional vibration mode around 70-80 Hz has a very similar behaviour as the in-phase mode around 40 Hz. That is, the natural frequency of the oscillation decreases and the amplitude increases with the loss of pressure, and the magnitude of these effects is quite similar to that for the in-phase mode. However, in contrast to the “component” model, the resonance peak for the “subsystem” model is definitely higher than the peak associated with the in-phase mode. Furthermore, this is more pronounced in the longitudinal acceleration data. Therefore, based on our results, we can suggest that the inclusion of the anti-phase mode in indirect TPMS seems to be definitely advantageous. This is especially true when, in addition to the data from the wheel angular velocity sensor, acceleration data are also available and the measured data are processed in a unified manner within an integrated system. This is a key finding of our work.

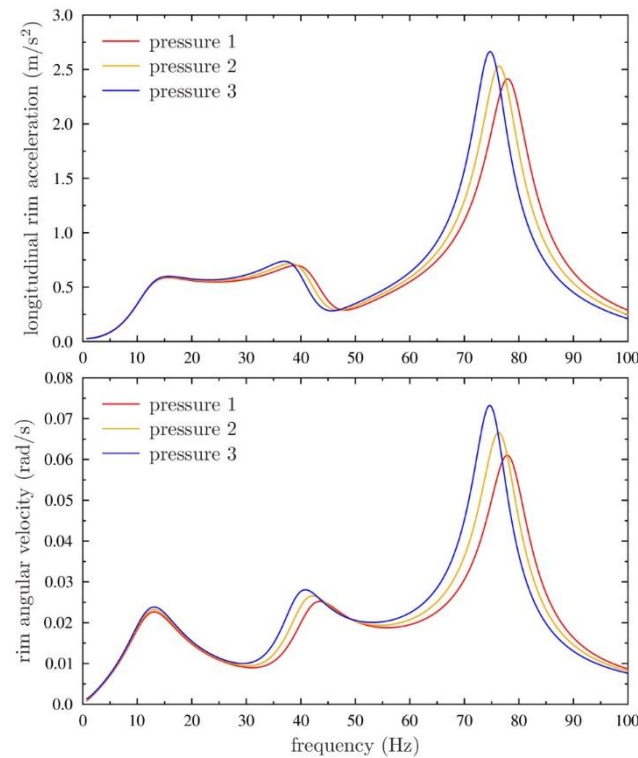


Figure 6. Amplitude spectrum of the wheel angular velocity (lower panel) and the longitudinal acceleration of the rim (upper panel) of the “component” model for a single cleat excitation at 36 km/h

Using the “subsystem” model in the simulation we determined the effect of axle elasticity on the sensitivity of the resonance peak to pressure loss. For this purpose, the generalized axle stiffness k_a is reduced from the initial value ($k_a = 350$ kN/m) to $k_a = 200$ kN/m and increased to $k_a = 500$ kN/m. With the new values for k_a , the “subsystem” model is simulated with a single cleat excitation at a speed

of 36 km/h and then the resulting vibration frequencies as well as the vibration amplitudes of the torsional longitudinal tyre mode are analysed.

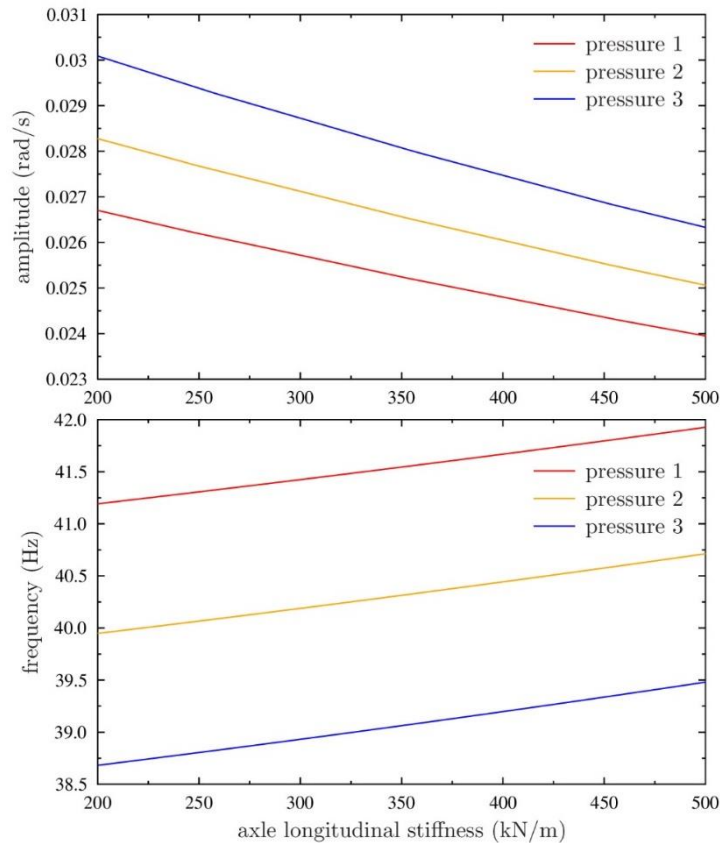


Figure 7. Vibration frequencies (lower panel) and vibration amplitudes (upper panel) of the torsional longitudinal tire mode with variation of the axle stiffness

The lower panel of Figure 7 compares the oscillation frequencies of the wheel angular rim acceleration with variation of the generalized axle stiffness k_a . It can be seen that the shift of vibration frequencies are approximately proportionally to k_a . In agreement with the measurements, the vibration frequencies increase with increasing axle stiffness. In the simulation, the vibration frequencies of the tyre longitudinal force and the wheel angular velocity increase by approx. 0.8 Hz with an increase in the axle stiffness from $k_a = 200$ kN/m to $k_a = 500$ kN/m, which corresponds to an increase of 150%. This shows that the sensitivity of the tyre properties with respect to a pressure loss is not significantly influenced by axle properties. Analogously, the upper panel of Figure 7 compares the oscillation amplitudes of the wheel angular velocity associated to the oscillation frequencies. This figure is important because the more pronounced the peak in the spectrum, the easier it is to detect the pressure loss. It can be seen that in the simulation, in correlation to the measurement (Pacejka, 2012), the

amplitudes decrease with increasing axle stiffness. However, in the case of the angular velocity, this effect is more pronounced compared to the measurement. Furthermore, it can be seen from the simulation results that the sensitivity with respect to the pressure-dependent amplitude variation slightly increases with decreasing axle stiffness.

6. Summary

We emphasize in this study that the important properties of the wheel vibrations in the frequency range that is important from the point of view of the indirect TPMS systems can be described sufficiently using a very simple minimal model based on the rigid ring tyre approximation. In order to better understand the pressure-dependent vibration behaviour of tyres, this phenomenon has been analysed by simulation to make some observations on the definition of the test procedure. For this purpose, the two simulation models “component” and „subsystem” are developed. Both models take into account the belt translation in longitudinal direction as well as the rotations around the transverse axis (y-axis) of belt and rim. In the “subsystem” model, the rim additionally has a translational degree of freedom with elastic coupling to the rigid environment to represent the interaction with the wheel suspension. The contact to the ground is realized in both models via a slip model according to the literature (Zegelaar, 1998). Based on the model characteristics (eigenfrequencies and eigenvectors) and time step simulations of the “component” model, the pressure dependence of the torsional longitudinal tyre mode is demonstrated. In this mode all degrees of freedom of the model oscillate in phase at 34.93 Hz (according to the “Pressure 1” parameterization). From the results it can be concluded that the effects of changing the conditions (such as tyre pressure variation) are equally observable in both the frequency and the amplitude of the resonance peak, which correlates with the measurement results on the test rigs and the road test.

From the model characteristics of the “subsystem” model, the interaction of the tyre oscillations with the longitudinal stiffness of the wheel suspension is evident. The first calculated mode at 11.77 Hz is characterized by the in-phase oscillation of all degrees of freedom of the model (i.e. longitudinal axle motion and tyre degrees of freedom) and results from the elastic suspension of the rim-coupled-to-axle masses. At 41.54 Hz, the second mode, which corresponds to the in-phase longitudinal torsional tyre mode, occurs at a significantly higher frequency compared to the “component” model. The torsional longitudinal mode of the “subsystem” model is characterized by the phase equality of the tyre degrees of freedom. Thus, even under the influence of the chassis elasticity, the strong coupling between the longitudinal acceleration of the rim and the wheel angular velocity is a characteristic feature of the longitudinal torsional tyre mode, even if it occurs at higher oscillation frequencies. Therefore the data from the wheel angular velocity produced for the ABS system can be effectively completed by accelerometer data to detect the pressure loss. The calculated correlation between the tyre vibration behavior and the axle elasticity shows a very good agreement with the measurement results.

The simulated single cleat crossings with the models show a high correlation to the measured data presented in the literature. The wheel angular velocity and the longitudinal acceleration of the rim are defined as output variables. We have found that the anti-phase mode of the torsional tyre vibrations shows a more pronounced peak together with the longitudinal acceleration data of the wheel, therefore it is important to take into consideration these frequencies in the indirect TPMS systems.

The “subsystem” model is also used to analyse the variation in the sensitivity of the tyre vibration behaviour to the pressure loss as a function of the longitudinal elasticity of the front axle suspension. It is shown that when the axle stiffness is varied, the oscillation frequencies of the torsional longitudinal tyre mode shift approximately in proportion with it, as in the measurements. The sensitivity of the natural

frequency of the tyre vibration with respect to a pressure loss is thus not influenced. In contrast, the vibration amplitude increases with decreasing tyre pressure the lower the axle stiffness. This effect is weakly supported by the measurements.

In summary, a tyre model with rigid ring as tyre belt is a suitable model approach to analyse both the correlation between tyre longitudinal acceleration or force and wheel angular velocity, and the interaction between tyre characteristics and axle elasticity. The tyre vibration behaviour relevant for the indirect tyre pressure monitoring systems can be reproduced with a very high correlation to the measured data using the selected model approach and the corresponding pressure-dependent parameterization.

References

- [1] Adnan, M. (2019). Technical Review: Indirect Tire Pressure Monitoring Systems and Tire Vibrations. *Tire Science and Technology*, 47(2), pp. 102–117.
<https://doi.org/10.2346/tire.18.460403>
- [2] Doria, A., Taraborrelli, L. (2016). Out-of-plane vibrations and relaxation length of the tyres for single-track vehicles. *Proceedings of the Institution of Mechanical Engineers, Part D: Journal of Automobile Engineering*, 230(5), pp. 609–622, <https://doi.org/10.1177/0954407015590703>
- [3] Durand-Gasselín, B., Dailliez, T., Mössner-Beigel, M., Knorr, S., Rauh, J. (2010). Assessing the thermo-mechanical TaMeTirE model in offline vehicle simulation and driving simulator tests. *Vehicle System Dynamics*, 48, pp. 211–229, <https://doi.org/10.1080/00423111003706730>.
- [4] Formentin, S., Onesto, L., Colombo, T., Pozzato, A., Savaresi, S. M. (2021). h-TPMS: a hybrid tire pressure monitoring system for road vehicles. *Mechatronics*, 74, pp. 102492.
<https://doi.org/10.1016/j.mechatronics.2021.102492>
- [5] Gallrein, A., Baecker, M., Gizatullin, A. (2013). Structural MBD Tire Models: Closing the Gap to Structural Analysis – History and Future of Parameter Identification. In *SAE 2013 World Congress & Exhibition*, SAE International, ISSN 0148-7191.
<https://doi.org/10.4271/2013-01-0630>
- [6] Hirschberg, W., Rill, G., Weinfurter, H. (2007). Tire model TMeasy. *Vehicle System Dynamics*, 45(sup1), pp. 101–119, <https://doi.org/10.1080/00423110701776284>
- [7] Kubba, A., Jiang, K., (2014). A comprehensive study on technologies of tyre monitoring systems and possible energy solutions. *Sensors*, 14(6), pp. 10306–10345.
<https://doi.org/10.3390/s140610306>
- [8] Gipser, M. (2016). FTire and puzzling tyre physics: teacher, not student. *Vehicle System Dynamics*, 54(4,SI), pp. 448–462, <https://doi.org/10.1080/00423114.2015.1117116>
- [9] Oertel, C., Wei, Y. (2012). Tyre rolling kinematics and prediction of tyre forces and moments: part I theory and method. *Vehicle System Dynamics*, 50(11), pp. 1673–1687.
<https://doi.org/10.1080/00423114.2012.694452>
- [10] Pacejka, H. (2012). *Tire and Vehicle Dynamics*. Oxford: Butterworth and Heinemann (3rd ed.)
<https://www.sciencedirect.com/book/9780080970165/tire-and-vehicle-dynamics>

- [11] Pfeffer, P. E., Hofer, K. (2002). Simple non-linear model for elastomer and hydro-mountings to optimise overall vehicle simulation. *ATZ worldwide*, 104, pp. 5–7.
<https://doi.org/10.1007/BF03224557>
- [12] Reiter, M., Wagner, J. (2010). Automated automotive tire inflation system – Effect of tire pressure on vehicle handling. *IFAC Proceedings Volumes*, 43(7), pp. 638–643.
<https://doi.org/10.3182/20100712-3-DE-2013.00013>
- [13] Schmeitz, A. J. C. (2004). A Semi-Empirical Three-Dimensional Model of the Pneumatic
- [14] Tyre Rolling over Arbitrarily Uneven Road Surfaces. PhD thesis, Delft University of Technology.
<https://repository.tudelft.nl/islandora/object/uuid%3Ad369bfac-4d8a-465c-a194-864bbe87d8e8>
- [15] Schmeitz, A. J. C., Besselink, I. J. M., Hoogh de, J., Nijmeijer, H. (2005). Extending the Magic Formula and SWIFT tyre models for inflation pressure changes. In *Reifen, Fahrwerk, Fahrbahn*, pp. 201–225, <https://research.tue.nl/en/publications/extending-the-magic-formula-and-swift-tyre-models-for-inflation-p>.
- [16] Sivaramakrishnan, S., Siramdasu, Y., Taheri, S. (2015). A New Design Tool for Tire Braking Performance Evaluations. *Journal of Dynamic Systems, Measurement, and Control* 137(7), p. 071013, <https://doi.org/10.1115/1.4029721>
- [17] Zegelaar, P. W. A. (1998). The dynamic response of tyres to brake torque variations
- [18] and road unevennesses. PhD thesis, Delft University of Technology.
<https://repository.tudelft.nl/islandora/object/uuid%3Ac623e3fc-b88a-4bec-804a-10bc7e94124>